Mechanism and Machine Theory 73 (2014) 91–100

Contents lists available at ScienceDirect

Mechanism and Machine Theory

journal homepage: www.elsevier.com/locate/mechmt

Dahl and LuGre dynamic friction models — The analysis of selected properties

T. Piatkowski *

University of Technology and Life Sciences, Faculty of Mechanical Engineering, Al. Prof. S. Kaliskiego 7, 85–789 Bydgoszcz, Poland

ARTICLE INFO

Article history:
Received 9 April 2013
Received in revised form 18 October 2013
Accepted 21 October 2013
Available online 17 November 2013

Keywords:
Dry friction
Friction hysteresis
Presliding displacement regime
Modelling
Simulation

ABSTRACT

The paper presents a method of determination of parameters for LuGre and Dahl dynamic friction models. The method involves the use of numeric optimisation, in which the objective function is a minimisation of the sum of squares of relative errors between the actual and modelled friction hysteresis courses. It was specified that the limiting value of the cycle time of the signal, forcing the relative motion, above which the simulation of friction hysteresis in the presliding regime is not dependent on the velocity of displacement. The analyses of numerical results indicated that the parameters of dynamic models have limited the scope of application in relation to the normal forces exerted on the kinematic friction pairs, as opposed to the static friction models.

1. Introduction

Friction is a phenomenon that commonly appears in almost all mechanical systems. The desire to explore this phenomenon has inspired researchers for many centuries. The first documented attempts of friction phenomenon modelling are attributed to Leonardo da Vinci. According to his research, the reaction force of friction is directly proportional to the normal force exerted on the body and the constant number of ¼, universal for all bodies. Years later it turned out that this constant (in modern models called the coefficient of friction) is correct for many combinations of materials of friction pairs. Despite a long history of research, the actual nature of the formation of the friction force has not been known yet. Ineffective compensated friction reaction forces lead to a limitation of technical devices functionality to such a degree that they become completely useless. Particular difficulties in friction force identification occur at very low velocities and displacements — typical for processes of precision positioning of the working device elements, such as robots, control systems of aircraft, aiming mechanisms, or machine tools. The author of the paper recognizes the seriousness of the problem of effective friction force defining due to the work experience; modelling, analysis and experimental verification of the sorting and positioning processes of objects stream with the use of nonprehensile manipulators. The issue of automatic, high-efficient positioning and sorting of unit loads occurs in the logistics centres in conveyor transport systems [1,14] or assembly lines. Friction, in these processes, is one of the dominant physical phenomena which determines the reliability and precision of programmed handling activities.

The source of dynamic nonlinearity causing the disturbances in receiving the assumed paths and errors in achieving programmed positions of working mechanisms are such phenomena as: stick–slip, break-away force, frictional lag or hysteresis of friction force in the range of presliding displacements.

Understanding the nature of friction, its modelling, identification and compensation are still current challenges faced by the researchers and designers of device drive control systems.

* Tel.: +48 52 3408145.
E-mail address: topiat@utp.edu.pl.

0094-114X/$ – see front matter © 2013 Elsevier Ltd. All rights reserved.
http://dx.doi.org/10.1016/j.mechmachtheory.2013.10.009

The purpose of the present paper is to propose a methodology for determining the parameters of Dahl and LuGre dynamic friction models which, in the available literature, is not presented and discussed in detail. There was also an analyis of an influence of body weight of kinematic friction pair on the efficiency and computing convergence of the models considered.

2. Contemporary friction models

The friction forces models proposed today can be divided into two major groups [6–8]:

- static models (derived from the Coulomb model) [8], e.g. models by Karnopp, Quinn, Kikuuwe, Awrejcewicz [4], and Wojewoda [18],
- dynamic models (derived from the Dahl model), e.g. LuGre model [6,19,13], Leuven model [12,16], and GMS model [3,5,10,11].

This division results from the modelling of friction at rest state.

In the static models, there is an assumption that in the standstill friction conditions the relative motion between the rubbing bodies does not occur and in the dynamic models — that small presliding displacements appear, at which the friction force is a function of displacement. This property has been confirmed by detailed experimental studies.

In the range of kinetic friction (when the bodies' relative velocity is above at about 0.003 m/s [1]), the two groups of models describe friction force similarly — as a function of slip velocity.

Static models, with a simpler structure and fewer parameters than in the dynamic models, are mainly dedicated to the study of friction pairs with significant slip velocities and a small number of transitions between standstill and kinetic friction states, especially when these transitions run in a rapid manner [1].

In case of modelling of precisely positioned mechanical systems with friction, it is necessary to use the dynamic friction models which consider both friction regimes [15,17]. Dynamic friction models, as opposed to the static models, allow for recreating processes occurring in standstill friction conditions and at very small as well as high sliding velocities. The main disadvantage of dynamic models is their complexity that results in being highly computation-wise time-consuming and in generating high calibration costs.

2.1. Dahl model

The Dahl model (1968) belongs to the earliest dynamic friction models; it was designed to simulate a symmetrical hysteresis loops observed in bearings subjected to sinusoidal excitations with small amplitudes. This model was applied e.g., in standard models of simulation in the aerospace industry [9].

The Dahl model is represented by the equation

$$\frac{dF}{dx} = \sigma_0 \operatorname{sgn}\left(1 - \operatorname{sgn}(v)\frac{F}{F_C}\right)\left|1 - \operatorname{sgn}(v)\frac{F}{F_C}\right|^{\delta_D} \tag{1}$$

which can be converted into form (2) — easier for the numerical implementation:

$$\begin{cases} F = \sigma_0 z \\ \dot{z} = v \operatorname{sgn}\left(1 - \operatorname{sgn}(v)\dfrac{\sigma_0 z}{F_C}\right)\left|1 - \operatorname{sgn}(v)\dfrac{\sigma_0 z}{F_C}\right|^{\delta_D} \end{cases} \tag{2}$$

where:

F friction force [N],
z state variable interpreted as elastic deformation of surface asperities of adjacent bodies [m] (Fig. 1),
$v = dx/dt$ sliding velocity [m/s],
x body displacement [m],
σ_0 asperity stiffness [N/m],

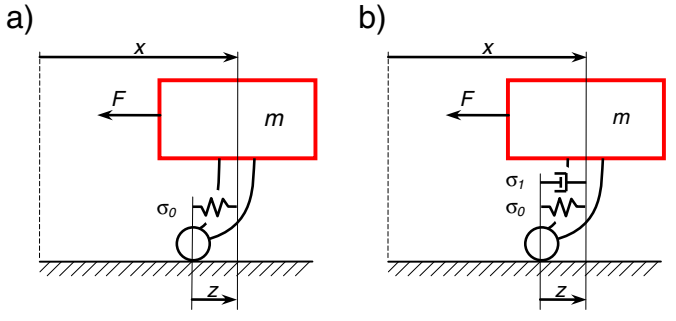

Fig. 1. Graphic representation of variable state z [21]: a) Dahl model, b) LuGre model.

δ_D coefficient determining the shape of the hysteresis loop [−],
F_C Coulomb friction [N].

Dependence (2) was obtained by multiplying both sides of Eq. (1) by dx/dt, then substituting $F = \sigma_0 z$ and divided by σ_0. The graphic representation of the state variable z is shown in Fig. 1.

2.2. LuGre model

The LuGre model came into being as a result of the Dahl model modification consisting in adoption of: the hysteresis shape coefficient $\delta_D = 1$, the Stribeck curve $s(v)$ and viscous damping coefficients σ_1 (Fig. 1b) and σ_2.

$$\begin{cases} F = \sigma_0 z + \sigma_1 \dot{z} + \sigma_2 v \\ \dot{z} = v - \dfrac{\sigma_0 |v|}{s(v)} z \\ s(v) = F_C + (F_S - F_C) \exp\left(-(v/v_s)^{\delta_{vs}}\right) \end{cases} \tag{3}$$

where:

$s(v)$ Stribeck's curve in the function of sliding velocity v [N]
σ_1, σ_2 damping coefficients that relate to the presliding and kinetic friction states, respectively [Ns/m],
v_s Stribeck's velocity [m/s],
$F_S = \mu_S N$, $F_C = \mu_C N$ static friction force and Coulomb friction force [N], respectively,
N normal force [N],
μ_S, μ_C friction coefficients [−],
δ_{vs} shape factor of Stribeck curve [−].

In the LuGre model, the Stribeck curve allows simulating two important properties of a friction phenomenon, observed experimentally; frictional lag and break-away force.

The Dahl and LuGre models are described by the dynamic equations systems that simultaneously model both friction regimes, presliding and sliding, in a continuous manner — with no need to use (between individual regimes) any switching functions.

3. Dahl and LuGre models parameters

The Stribeck's curve parameters (required in the LuGre model), which describe the friction phenomenon in kinetic friction conditions (Fig. 2a), are taken from [2] ($F_S = 55.3$ N, $F_C = 46.49$ N, $v_s = 1.646 \times 10^{-3}$ m/s, $\delta_{vs} = 0.791$). Furthermore, from the analysis of Fig. 2a one can see that the damping coefficient σ_2, relating to the kinetic friction state is zero ($\sigma_2 = 0$). Parameters concerning the friction at rest state ($\sigma_0, \sigma_1, \delta_D$) are determined via numerical optimization (in Matlab environment), based on the graph given in Fig. 2b. This graph presents the hysteresis loop of the friction force recorded during the experimental testing [9], obtained in the range of presliding displacements. When testing, an external force F_{ext} (applied to the frictional pair of bodies) was slowly ramped up to 90% of F_S (when displacement $x_{max} = 0.891 \times 10^{-4}$ [m]), then slowly ramped down to 90% of F_S and later — slowly ramped up to 90% of F_S again.

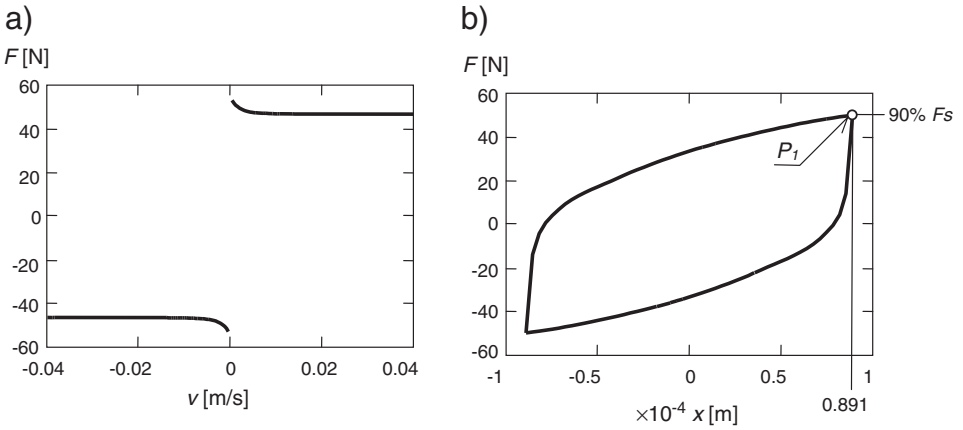

Fig. 2. Results of experimental tests of friction according to [2]: a) Stribeck's curve ($F_S = 55.3$ N, $F_C = 46.49$ N, $v_s = 1.65 \cdot 10^{-3}$ m/s, $\delta_{vs} = 0.791$), b) hysteresis loop of friction force in the range of presliding displacement; P_1 — hysteresis point in which the maximum frictional force F is recorded.

3.1. Friction hysteresis parameters determination methodology in the presliding displacement regime

3.1.1. LuGre model

The properties of the LuGre model in the range of presliding displacements are described by two parameters: σ_0 and σ_1. Since parameter σ_1 is dependent on σ_0 (the selection of σ_1 is given in chapter 4), to identify the LuGre model, it is necessary to determine only one parameter: σ_0. It can be determined, with good results, by solving numerically the equation

$$\hat{F}_{\max}(\sigma_0) - F_{\max} = 0 \tag{4}$$

where: $\hat{F}_{\max}(\sigma_0)$, $F_{\max}$ — friction forces determining point P_1 in Fig. 2b, obtained respectively: during numerical simulation and while experimental testing.

To solve Eq. (4), the *fzero* function, available in standard library of Matlab, is applied. An algorithm of this function comprises a combination of methods: bisection, secant, and inverse quadratic interpolation. During the search for a solution, and the adequate simulation of the friction model, the input signal is applied (forcing presliding displacement) according to the graph shown in Fig. 5a, in which the maximum value corresponds to the maximum displacement registered in Fig. 2b ($x_{max} = 0.891 \times 10^{-4}$ m).

An essential impact on the success of the search for a solution is the type of the algorithm applied to solve nonlinear friction models. This paper adopts *ode23tb* function (implementing an implicit Runge–Kutta formula), dedicated to integrate the so-called rigid equations. Based on the results of the preliminary tests, the integration parameters were assumed: $RelTol = 10^{-6}$, $AbsTol = 10^{-12}$.

3.1.2. Dahl model

In the Dahl model, the static friction force hysteresis is defined by two parameters: σ_0 and δ_D. In order to determine those parameters, it is necessary to use numerical optimization with two decision variables. When solving the optimization task, the simulated hysteresis course of friction force, represented as a function of time in Fig. 3b — curve 1, is adjusted to the actual course (Fig. 3b — curve 3).

The minimized criterion of evaluation is the sum of the squares of relative errors between the actual and modelled courses of hysteresis:

$$\min Q(X) = \sum_{i=1}^{n} \left(\frac{\hat{F}_i - F_i}{\hat{F}_i} \right)^2 \tag{5}$$

where:

$X = [\sigma_0, \delta_D]$ vector of decision variables,
$\hat{F}_i, F_i$ *ith*-value of the friction force determined during numerical simulation and real tests, respectively,
$n = T/\Delta t$ number of discretization steps,
T time cycle of hysteresis loop [s],
$\Delta t = 0.01$ s discretization step of hysteresis loop.

It was assumed that the constraint of the optimization task is the requirement of overlapping the points P_1 of the friction hysteresis determined during the simulation and experimental tests (Fig. 3):

$$\hat{F}_{\max}(\sigma_0, \delta_D) - F_{\max} = 0. \tag{6}$$

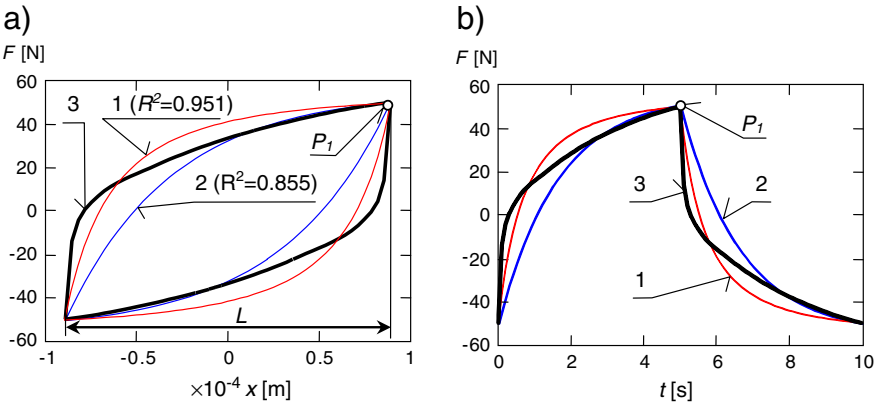

Fig. 3. Hysteresis loops of friction force as a function of: a) displacement, b) time; 1 — the Dahl model, 2 — the LuGre model, 3 — experimental test [2]; $\sigma_{0LuGre} = 946160$ N/m, $\sigma_{0Dahl} = 1592200$ N/m, $\delta_D = 1.52$, L — hysteresis span, P_1 — hysteresis point in which the maximum frictional force F is recorded.

Calculations were performed using the *patternsearch* function available in the Matlab Optimization Toolbox. The function is designated to solve nonlinear optimization tasks with multiple decision variables and constraints. The *patternsearch* function represents the family that does not require the gradient of the problem to be optimized, thus the objective function or constraints do not have to be continuous and differentiable. During the preliminary tests we also used the *fmincon* function with the SQP algorithm belonging to the family of gradient methods. The tests demonstrated, however, that in the present application *patternsearch* function shows greater convergence than *fmincon*.

While searching for the minimum of the objective function, the following was adopted: $TolMesh = 10^{-12}$, $MaxFunEvals = 10^4$.

4. Numerical research and results analysis

The results of numerical optimization are shown in (Figs. 3–6). As for the Dahl model application, the real course of the hysteresis loop is mapped more accurately ($R^2 = 0.951$, $\sigma = 7.6902$; where: R^2 – coefficient of determination, σ – standard deviation) – than in the LuGre model ($R^2 = 0.855$, $\sigma = 13.187$), which is due to the Dahl model parameter δ_D, responsible for the hysteresis shape correction. A side effect of the use of that parameter is a greater number of iterations l performed during simulation: for the Dahl model $l = 138$, and in the LuGre model $l = 78$ – Fig. 4b, when $\xi = 0$.

While testing the influence of parameter σ_1 on the LuGre model properties, this parameter is expressed by the dimensionless relative damping ξ (damping degree). Assuming a linear elastic-damping coupling between the surface asperities of the bodies (Fig. 1b), relative damping takes the form:

$$\xi = h/\omega_o \tag{7}$$

where:

$h = 0.5\sigma_1/m$ unitary damping [rad/s].
$\varpi_0 = \sqrt{\sigma_0/m}$ natural frequency [rad/s].

The parameter σ_1 of the LuGre model has no essential influence on the course of the friction hysteresis loop (Fig. 4a); it stabilizes the integration process of friction model equations. According to Fig. 4b, the integration process is most effective when the relative damping (in the friction model) assumes a value of about $\xi = 0.5$.

From the analysis of Fig. 5b it follows that in the Dahl model (marked with a dashed line), cycle time T of input signal does not influence the maximum value of the friction force. The LuGre model (marked with solid line – Fig. 5b) is just the opposite: the shorter cycle time T, the smaller force F. This effect is related to the property of the LuGre model and its ability to simulate the phenomenon of breakaway force (Fig. 5d – feature registered during experimental testing [6], not available for the Dahl model). From the comparison of Figs. 5b,c and 6 (Fig. 6 has been developed based on [6]) one can see that the influence of period T on the friction force is not constant; it depends on the parameters of the simulated model. The course of the friction hysteresis is particularly susceptible to the speed of change of the input signal, when $T < 10$ s (Figs. 5b,c and 6). For that reason, the parameters of dynamic friction models describing the friction hysteresis loop in the range of presliding displacements should be determined using a low speed of input signal change, for example $T > 10$ s (which according to Figs. 5c and 6b result in the quotient $F_{LuGre} / F_{Dahl} \cong 0.99$).

A characteristic feature of static friction models is that when the friction coefficient is determined for a given pair of bodies, it is theoretically correct for any normal force exerted on these bodies. The friction force is proportional to the coefficient of friction and normal forces, without any computational obstacles.

As for dynamic friction models, it is different; the friction parameters determined for the one load conditions of normal force cannot be uncritically used to calculate the friction force for any other arbitrary normal forces.

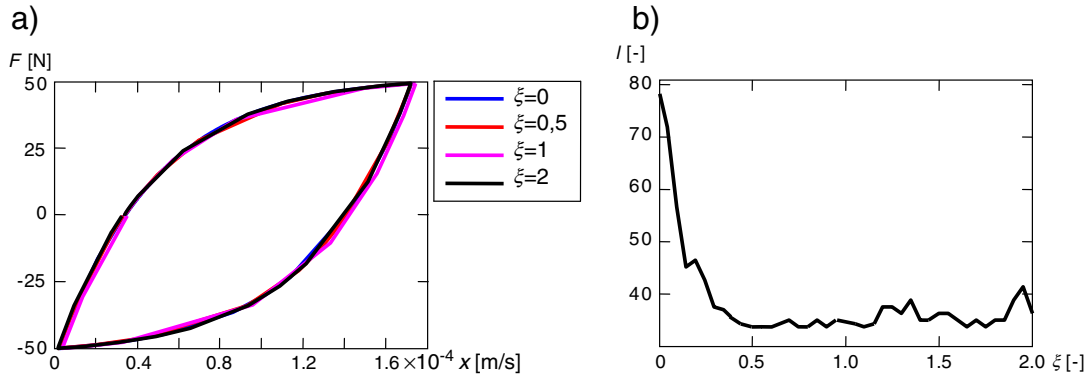

Fig. 4. Influence of relative damping ξ in the LuGre model on: a) friction force loop path, b) iteration number; $\xi = h/\omega_0, h = \sigma_1/2\ m, \omega_0 = (\sigma_0/m)^{0,5}, \sigma_0$ – stiffness of the surface asperities, σ_1 – damping coefficient; for the Dahl model $l = 138$.

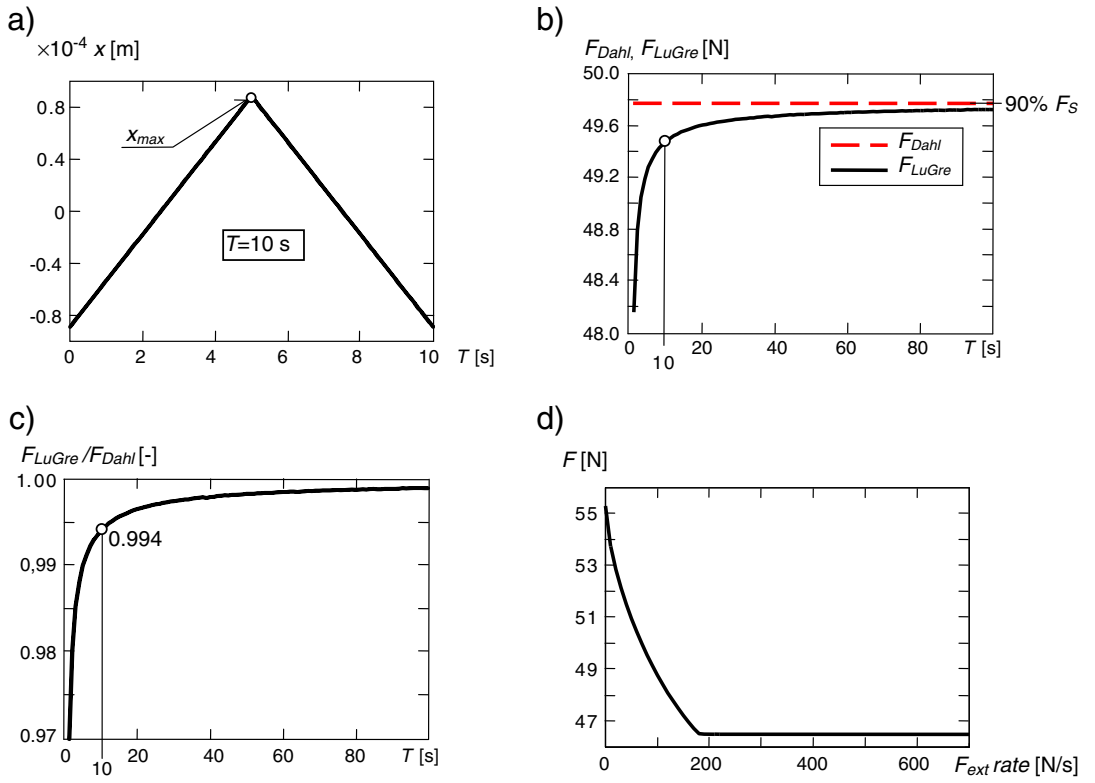

Fig. 5. Influence of the rate of change of the input signal on the properties of dynamic friction models: a) one cycle of input signal, b) an influence of cycle time T of input signal on maximum friction force value according to the Dahl and LuGre models, c) quotient F_{LuGre}/F_{Dahl} according to Fig. 5b, d) the friction force upon the transition from static to kinetic friction vs. increase in external force (break-away force).

This problem is given in Figs. 7–12 demonstrating the simulation of the friction force exerted on mass m which moved onto the horizontal ground.

It was assumed that the movement of the body in the presliding displacements range is caused by an external force:

$$F_{ext} = 0.9F_S sin(\omega t) \tag{8}$$

where:

$\omega = 2\pi/T$ frequency of external force [rad/s],
$T = 10$ s input signal period.

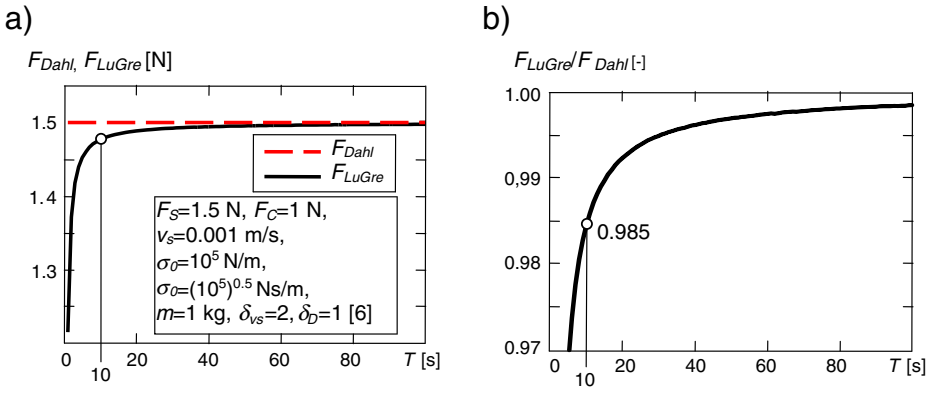

Fig. 6. Properties of the LuGre and Dahl models according to data [6]: a) influence of cycle time T of input signal on maximum friction force value, b) quotient F_{LuGre}/F_{Dahl} according to Fig. 6a; $F_S = 1.5$ N; $F_C = 1$ N; $v_s = 0.001$ m/s; $\sigma_0 = 10^5$ N/m, $\sigma_1 = (10^5)^{0.5}$ Ns/m, $m = 1$ kg, $\delta_{vs} = 2$, $\delta_D = 1$.

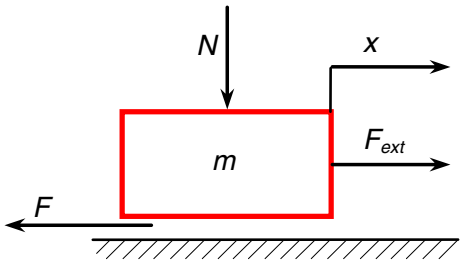

Fig. 7. Diagram of the forces exerted on the object.

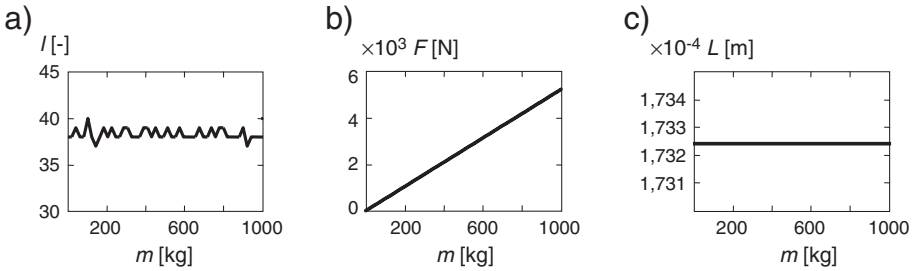

Fig. 8. Influence of the body mass on the simulation result of friction phenomenon, when $\sigma_0 =$ f(m), $\omega_0 =$ const: a) number of iterations, b) friction force, c) span of hysteresis loop; $m \in \langle 0.001;\ 1000 \rangle$ kg, the LuGre model.

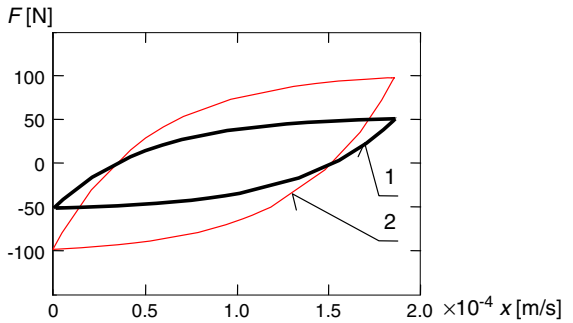

Fig. 9. Friction hysteresis loop in the presliding regime determined for: 1 — $m = 10$ kg, 2 — $m = 20$ kg; $\sigma_0 = f(m)$, $\omega_0 =$ const $= 307.597$ rad/s, the LuGre model.

In addition, it was also assumed that mass m applied while determining the parameters presented on charts in Fig. 3 is $m = 10$ kg ($N = mg$, where g — gravity acceleration).

The conclusions from the results analysis for a simple mechanical system simulation (mass set into motion on the horizontal and rough surface, Fig. 7) are general; they are valid for more complex systems. The model proposed, despite its simplicity, allows the identification of the essential relationships that exist between a clamping force, displacement, velocity of displacement,

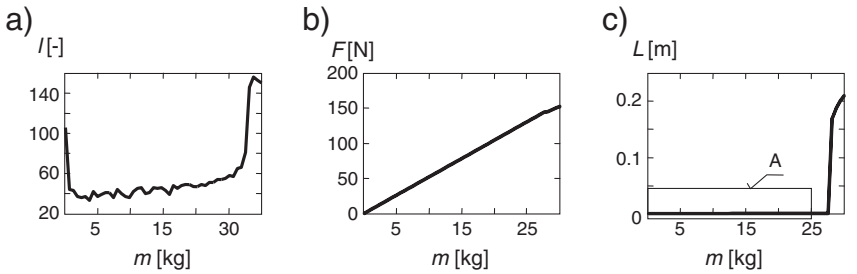

Fig. 10. Influence of mass m on the simulation result of friction phenomenon when $\sigma_0 =$ const, $\omega_0 = f(m)$: a) the number of iterations, b) force of friction, c) span of the hysteresis loop; $m \in \langle 0.1;\ 35 \rangle$ kg, A — detail shown in Fig. 11a, the LuGre model.

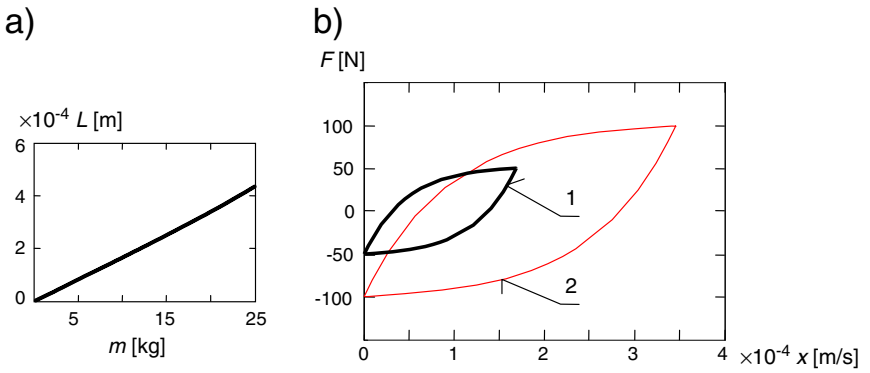

Fig. 11. Friction hysteresis in the function of body mass: a) magnified detail A in Fig. 10c ($m\epsilon\langle 0.1; 25\rangle$ kg), b) hysteresis loops for $m = 10$ kg (curve 1) and $m = 20$ kg (curve 2); $\omega_0 = f(m)$, $\sigma_0 = \text{const} = \sigma_{0LuGre} = 946160$ N/m, the LuGre model.

external force and the reaction of friction force. The analysis of arbitrarily complex mechanical systems with friction always boils down to the need to investigate the correlation of the so called chosen quantities. In case of high velocity of slip, each dynamic friction model works as the static models (Coulomb-based models).

Based on the LuGre model, the natural frequency of the dynamic system, shown in Fig. 7, can be expressed as dependence:

$$\varpi_o = \sqrt{\sigma_0/m} = 307.597\,[\text{rad/s}] \tag{9}$$

where:

$$\sigma_0 = \sigma_{0LuGre} = 946160\,\text{N/m}, m = 10\,\text{kg}$$

The kinetic and static friction coefficients (based on the Coulomb model) are:

$$\mu_C = F_C/mg = 0.474 \quad \mu_S = F_S/mg = 0.564 \tag{10}$$

where:

$F_S = 55.3$ N static friction force [2],
$F_C = 46.49$ N kinetic friction force [2].

Figs. 8 and 9 show the properties of the LuGre model expressed in the function of body mass, at the assumption that:

$$\sigma_0(m) = m\omega_0^2 \tag{11}$$

$$F_C(m) = mg\mu_C, F_S(m) = mg\mu_S \tag{12}$$

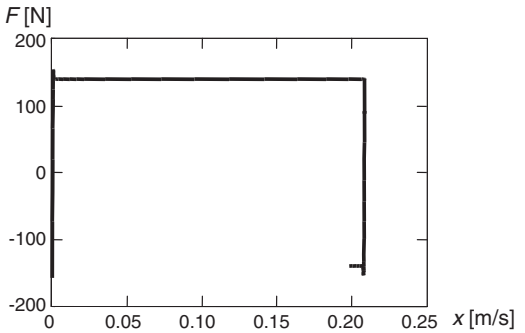

Fig. 12. Chart of friction force in the range of presliding displacement for $\sigma_0 = \text{const} = \sigma_{0LuGre} = 946160$ N/m and $m = 30$ kg – hysteresis loop is not closed; the LuGre model.

$$\omega_0 = \text{const} = 307.597 \text{ rad/s}. \tag{13}$$

From the analysis of Figs. 8 and 9 one can see that if we consider $\omega_o = \text{const}$ (dependences (11 ÷ 13)), the properties of the LuGre and Coulomb models are comparable in the wide range of changes of body mass $m \epsilon \langle 0.001; 1000 \rangle$ kg; friction force F is a linear function of mass m (Fig. 8b), the number of iterations l performed during calculation reaches almost a constant value (Fig. 8a, $l \cong const$), as well as the span of the hysteresis loop (Figs. 8c and 9, $L = const$).

Other relationships between body mass m and the properties of the LuGre model appear if we accept the constant stiffness $\sigma_0 = \text{const}$:

$$\sigma_0 = \text{const} = \sigma_{0LuGre} = 946160 \text{ N/m} \tag{14}$$

$$F_S(m) = mg\mu_S,\ F_C(m) = mg\mu_C \tag{15}$$

$$\varpi_o(m) = \sqrt{\sigma_0/m}. \tag{16}$$

The friction force determination in the whole range of body mass $m \epsilon \langle 0.1; 35 \rangle$ kg is not possible to obtain (Figs. 10–12). Difficulties in the integration of the LuGre model equations appear when the value of mass m significantly differs from mass $m = 10$ kg for which the friction coefficients (10) were determined. The failure of the simulation is revealed by a sharp increase in iteration number of calculations (Fig. 10a), a sudden change in friction force (Fig. 10b) and an increase in span L of friction hysteresis (Fig. 10c) associated with a lack of the loop closure (Fig. 12). The instability, typical of rigid differential equations [21], is caused by terms of equations that lead to a rapid change in the solution. The change of mass causes a change of natural frequency of the system $\omega_o = (\sigma_0/m)^{0.5}$. In addition there also exists the element F_{ext} forcing the mass displacement at constant frequency $\omega = 2\pi/T$ ($T = 10$ s). The problem with the equation integration can be explained by the appearance of large discrepancies between the values ω_o and ω; both when m is very low or very high.

For the range of mass m, at which the logical courses of friction forces were obtained, span L of the closed hysteresis loops (Fig. 11b) is a linear function of mass m (Fig. 11a).

Among the two theoretical scenarios of the determination of friction force F in a function of body mass m, the first variant, determining linear stiffness σ_0 in the function of mass m (11 ÷ 13), is executed. This is evidenced by the results of the experimental tests published, for example, in [22], in which a linear dependence of stiffness σ_0 on normal force N is shown (Fig. 13). The effect can be accounted for by the fact that with an increase in force N, there increases the actual area of body adherence and the associated stiffness of coupling between asperities. The results shown in Fig. 13, however, refer to the small range of changes of normal force N, which do not fully confirm the behaviour of linear rigidity σ_0 for significantly higher loads.

5. Summary

- The paper presents the methodology for determining the parameters of the Dahl and LuGre dynamic models.
- Parameters describing the friction hysteresis in the range of presliding displacements should be determined with the use of low velocity of input signal course in order to make the simulation results of friction hysteresis independent from cycle time T. Cycle time $T > 10$ s of input signal should be considered as the initial value, recommended during preliminary testing which, having been verified, can be adapted to the specific parameters of the system analysed.
- The friction parameters determined for one external loading should not be uncritically used for other arbitrary normal forces exerted on the kinematic friction pairs. Friction parameters are adequate for the normal forces that are in close vicinity to the loading for which the friction model parameters were identified. According to the available literature, presenting the results of experimental tests, one should consider that in the range of small changes of normal force exerted on the body, the stiffness of surface asperities is linear.

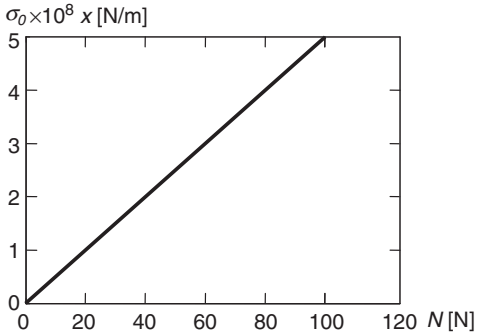

Fig. 13. Chart of stiffness coefficient σ_0 in the function of normal force N, developed based on experimental research according to [23].

References

[1] T. Piatkowski, Analysis of translational positioning of unit loads by directionally-oriented friction force fields, Mechanism and Machine Theory, 46, Elsevier, 2011. 201–217.
[2] V. Lampaert, J. Swevers, F. Al.-Bender, Experimental comparison of different friction model for accurate low-velocity cracking, Proceedings of the 10th Mediterranean Conference on Control and Automation — MED 2002 Lisbon, Portugal, July 9–12, 2002, (10 pp.).
[3] F. Al-Bender, V. Lampaert, J. Swevers, The generalized Maxwell-slip model: a novel model for friction simulation and compensation, IEEE Trans. Autom. Control 50 (11) (2005) 1883–1887.
[4] J. Awrejcewicz, D. Grzelczyk, Y. Pyryev, A novel friction modelling and its impact on differential equations computation and Lyapunov exponents estimation, Vibromechanika, J. Vibroengineering 10 (4) (2008) 475–482.
[5] M. Boegli, T. De Laet, J. De Schutter, J. Swevers, A smoothed GMS friction model for moving horizon friction state and parameter estimation, The 12th IEEE International Workshop on Advanced Motion Control, Sarajevo, Bosnia and Hercegovina, 2012, (6 pp.).
[6] C. Canadus de Wit, H. Olson, K.J. Åström, P. Lischinsky, A new model for control of systems with friction, IEEE Trans. Autom. Control 40 (3) (1995) 419–425.
[7] C.Ch. Casanova, E.R. De Pieri, U.F. Moreno, E.B. Castelan, Friction compensation in flexible joints robot with GMS model: identification, control and experimental results, Proceedings of the 17th World Congress, The International Federation of Automatic Control, Seoul, Korea, 2008, (11793–1198).
[8] R. Kikuuwe, N. Takesue, A. Sano, H. Mochiyama, H. Fujimoto, Fixed-step friction simulation: from classical Coulomb model to modern continuous models, Proceedings of IEEE/RSJ International Conference on Intelligent Robots and Systems, Edmonton, 2–6 Aug., Canada, 2005, pp. 3910–3917.
[9] V. Lampaert, J. Swevers, F. Al-Bender, Comparison of model and non-model based friction compensation techniques in the neighbourhood of pre-sliding friction, Proceedings of the 2004 American Control Conference, 2004, pp. 1121–1126.
[10] V. Lampaert, F. Al-Bender, J. Swevers, A generalized Maxwell-slip friction model appropriate for control purposes, Proceedings of International Conference PhysCon 2003, 20–22 August, 2003, pp. 1170–1177, (St. Petersburg).
[11] V. Lampaert, J. Swevers, F. Al-Bender, Experimental characterization of dry friction at low velocities on a developed tribometer setup for macroscopic measurements, Tribol. Lett. 16 (2004) 95–105.
[12] V. Lampaert, J. Swevers, F. Al-Bender, Modification of the Leuven integrated friction model structure, IEEE Trans. Autom. Control 47 (4) (2002) 683–687(32 pp.).
[13] A.K. Padthe, J. Oh, D.S. Bernstein, On the LuGre model and friction-induced hysteresis, Proceedings of the 2006 American Control Conference, Minneapolis, Minnesota, USA, June 14–16, 2006, pp. 3247–3252.
[14] T. Piatkowski, Analysis of translational positioning of unit loads by directionally-oriented friction force fields, Mechanism and Machine Theory, 46, Elsevier, 2011. 201–217.
[15] D.D. Rizos, S.D. Fassois, Friction identification based upon the LuGre and Maxwell slip models, IEEE Trans. Control Syst. Technol. 17 (1) (2009) 153–160.
[16] J. Swevers, F. Al-Bender, C.G. Ganseman, T. Prajogo, An integrated friction model structure with improved presliding behaviour for accurate friction compensation, IEEE Trans. Autom. Control 45 (4) (2000) 675–686.
[17] T. Tjahjowidodo, F. Al-Bender, H. Van Brussel, W. Symens, Friction characterization and compensation in electro-mechanical systems, J. Sound Vib. 308 (2007) 632–636.
[18] J. Wojewoda, Hysteretic effects in dry friction, Monograph 366, Technical University of Lodz, 2008. (124 pp.).
[19] J. Liang, S. Fillmore, O. Ma, An extended bristle friction force model with experimental validation, Mech. Mach. Theory 56 (2012) 123–137.
[20] P. Dupont, B. Armstrong, V. Hayward, Elasto-plastic friction model: contact compliance and stiction, Proceedings of the American Control Conference, 2, 2000, pp. 1072–1077.
[21] K.C. Park, An improved stiffly stable method for direct integration of nonlinear structural dynamic equations, J. Appl. Mech. 42 (2) (1975) 464–470.
[22] F. Altpeter, Friction modelling, identification and compensation, (Thesis 1988) Ecole Polytechnique Federale De Lausanne1999. (149 pp.).